Synthesis, Characterization, and Ethylene Oligomerization of Nickel Complexes Bearing N-((Pyridin-2-yl)methylene)quinolin-8-amine Derivatives†

ARTICLE *in* ORGANOMETALLICS · AUGUST 2007

Impact Factor: 4.13 · DOI: 10.1021/om700440v

7 AUTHORS, INCLUDING:

Wenhua Sun
Chinese Academy of Sciences
319 PUBLICATIONS **6,114** CITATIONS
SEE PROFILE

Yan Li
Dalian University of Technology
676 PUBLICATIONS **9,513** CITATIONS
SEE PROFILE

Synthesis, Characterization, and Ethylene Oligomerization of Nickel Complexes Bearing *N*-((Pyridin-2-yl)methylene)quinolin-8-amine Derivatives†

Wen-Hua Sun,* Kefeng Wang, Katrin Wedeking, Dongheng Zhang, Shu Zhang, Jingjing Cai, and Yan Li

Key Laboratory of Engineering Plastics and Beijing National Laboratory for Molecular Sciences, Institute of Chemistry, Chinese Academy of Sciences, Beijing 100080, People's Republic of China

Received May 4, 2007

A series of nickel complexes ligated by *N*-((pyridin-2-yl)methylene)quinolin-8-amine derivatives were synthesized by one-pot reaction of 8-aminoquinolines, 1-(pyridine-2-yl) ketones, and nickel halides and characterized by elemental and spectroscopic analyses along with X-ray diffraction analyses. These nickel complexes exhibit two kinds of structures, namely, dimeric with octahedral-coordinated geometry and monomeric with distorted trigonal-bipyramidal geometry, in their solid states. Activated by Et_2AlCl, these Ni(II) complexes exhibited good to high catalytic activities for ethylene oligomerization, and activity up to 4.9×10^7 g mol^{-1}(Ni) h^{-1} was observed in the catalytic system with Cy_3P as auxiliary ligand. The steric and electronic influence of the substituents as well as the influence of different catalytic conditions was carefully investigated. In particular, the correlations between reactivity and auxiliary R_3P ligands were examined.

1. Introduction

The modern chemical industry has much reliance on α-olefins, and development of new catalysts for oligomerization and polymerization of ethylene is of great interest to academic and industrial pursuits. One major industrial process in ethylene oligomerization, the Shell higher olefin process (SHOP), employs nickel complexes as catalyst.[1] Over the past decade, research into nickel complexes as catalysts for olefin reactivity has attracted much attention due to the substantial breakthrough by the group of Brookhart with the development of highly active catalysts for ethylene polymerization.[2] The important progress of ethylene reactivity promoted by nickel complexes is reflected by the recent review articles.[3] Ethylene reactivity includes two competitive reactions, oligomerization and polymerization, with the mechanistic difference of chain termination and propagation. Recent challenges in the application of nickel complexes in ethylene oligomerization are improving their catalytic activity and selectively for the formation of α-olefins and controlling the polymer properties of produced polymers. From an academic view, the fundamental points in designing novel complexes as good homogeneous catalysts are based on designing and synthesizing suitable ligands to provide a conductive environment for the coordination of the olefin to the metal center. Besides the well-explored SHOP catalyst, a neutral Ni complex ligated by P^O[4] ligands in a bidentate manner, numerous Ni complexes ligated by bidentate N^O,[5] P^N,[6] and N^N,[2,7] and tridentate ligands such as N^N^O,[8] N^P^N (**A**),[9] P^N^P (**B**),[10a] P^N^N (**C**[10a] and **D**[10b]), and N^N^N (**E**[11] and **F**[12]) have been reported (Scheme 1). Although these catalysts still have some disadvantages for commercialization in a short period, some nickel catalytic systems showed very good activities for ethylene reactivity, and further investigation will be promising for both industrial and academic developments.

† Dedicated to Prof. Heinz Berke on the occasion of his 60th birthday.

* Corresponding author. Tel: +86 10 62557955. Fax: +86 10 62618239. E-mail: whsun@iccas.ac.cn.

(1) (a) Keim, W.; Kowaldt, F. H.; Goddard, R.; Krüger, C. *Angew. Chem., Int. Ed. Engl.* **1978**, *17*, 466−467. (b) Keim, W.; Behr, A.; Limbäcker, B.; Krüger, C. *Angew. Chem., Int. Ed. Engl.* **1983**, *22*, 503.

(2) (a) Johnson, L. K.; Killian, C. M.; Brookhart, M. *J. Am. Chem. Soc.* **1995**, *117*, 6414−6415. (b) Johnson, L. K.; Mecking, S.; Brookhart, M. *J. Am. Chem. Soc.* **1996**, *118*, 267−268. (c) Killian, C. M.; Tempel, D. J.; Johnson, L. K.; Brookhart, M. *J. Am. Chem. Soc.* **1996**, *118*, 11664−11665.

(3) (a) S. D. Ittel, Johnson, L. K.; Brookhart, M. *Chem. Rev.* **2000**, *100*, 1169−1203. (b) Mecking, S. *Angew. Chem., Int. Ed.* **2001**, *40*, 534−540. (c) Gibson, V. C.; Spitzmesser, S. K. *Chem. Rev.* **2003**, *103*, 283−315. (d) Speiser, F.; Braustein, P.; Saussine, L. *Acc. Chem. Res.* **2005**, *38*, 784−793. (e) Zhang, W.; Zhang, W.; Sun, W.-H. *Prog. Chem.* **2005**, *17*, 310−319. (f) Jie, S.; Zhang, S.; Sun, W.-H. *Petrochem. Tech. (Shiyou Huagong)* **2006**, *35*, 295−300. (g) Sun, W.-H.; Zhang, D.; Zhang, S.; Jie, S.; Hou, *J. Kinet. Catal.* **2006**, *47*, 278−283.

(4) (a) Keim, W. *Angew. Chem., Int. Ed. Engl.* **1990**, *29*, 235−244. (b) Pietsch, J.; Braunstein, P.; Chauvin, Y. *New J. Chem.* **1998**, *22*, 467−472. (c) Heinicke, J.; He, M.; Dal, A.; Klein, H.-F.; Hetche, O.; Keim, W.; Flörke, U.; Haupt, H.-J. *Eur. J. Inorg. Chem.* **2000**, 431−440. (d) Heinicke, J.; Köhler, M.; Peulecke, N.; Keim, W. *J. Catal.* **2004**, *225*, 16−23. (e) Braunstein, P.; Chauvin, Y.; Mercier, S.; Saussine, L. *C. R. Chim.* **2005**, *8*, 31−38. (f) Kuhn, P.; Sémeril, D.; Jeunesse, C.; Matt, D.; Neuburger, M.; Mota, A. *Chem.−Eur. J.* **2006**, *12*, 5210−5219. (g) Kuhn, P.; Sémeril, D.; Matt, D.; Chetcuti, M. J.; Lutz, P. *J. Chem. Soc., Dalton Trans.* **2007**, 515−528. (h) Klabunde, U.; Ittel, S. D. *J. Mol. Catal.* **1987**, *41*, 123−134.

(5) (a) Wang, C.; Friedrich, S.; Younkin, T. R.; Li, R. T.; Grubbs, R. H.; Bansleben, D. A.; Day, M. W. *Organometallics* **1998**, *17*, 3149−3151. (b) Younkin, T. R.; Connor, E. F.; Henderson, J. I.; Friedrich, S. K.; Grubbs, R. H.; Bansleben, D. A. *Science* **2000**, *287*, 460−462. (c) Carlini, C.; Isola, M.; Liuzzo, V.; Galletti, A. M. R.; Sbrana, G. *Appl. Catal., A* **2002**, *231*, 307−320. (d) Wang, L.; Sun, W.-H.; Han, L.; Li, Z.; Hu, Y.; He, C.; Yan, C. *J. Organomet. Chem.* **2002**, *650*, 59−64. (e) Wu, S.; Lu, S. *Appl . Catal., A* **2003**, *246*, 295−301. (f) Zhang, D.; Jie, S.; Zhang, T.; Hou, J.; Li, W.; Zhao, D.; Sun, W.-H. *Acta Polym. Sin.* **2004**, *5*, 758−762. (g) Sun, W.-H.; Zhang, W.; Gao, T.; Tang, X.; Chen, L.; Li, Y.; Jin, X. *J. Organomet. Chem.* **2004**, *689*, 917−929. (h) Hu, T.; Tang, L.-M.; Li, X.-F.; Li, Y.-S.; Hu, N.-H. *Organometallics* **2005**, *24*, 2628−2632.

(6) (a) Keim, W.; Killat, S.; Nobile, C. F., Suranna, G. P.; Englert, U.; Wang, R.; Mecking, S.; Schröder, D. L. *J. Organomet. Chem.* **2002**, *662*, 150−171. (b) Sun, W.-H.; Li, Z.; Hu, H.; Wu, B.; Yang, H.; Zhu, N.; Leng, X.; Wang, H. *New J. Chem.* **2002**, *26*, 1474−1478. (c) Speiser, F.; Braunstein, P.; Saussine, L.; Welter, R. *Organometallics* **2004**, *23*, 2613−2624. (d) Speiser, F.; Braunstein, P.; Saussine, L. *Organometallics* **2004**, *23*, 2625−2632. (e) Speiser, F.; Braunstein, P.; Saussine, L. *Organometallics* **2004**, *23*, 2633−2640. (f) Speiser, F.; Braunstein, P.; Saussine, L.; Welter, R. *Inorg. Chem.* **2004**, *43*, 1649−1658. (g) Weng, Z.; Teo, S.; Hor, T. S. A. *Organometallics* **2006**, *25*, 4878 − 4882.

10.1021/om700440v CCC: $37.00
Publication on Web 08/11/2007

Scheme 1. Nickel Catalysts Bearing Tridentate Ligands

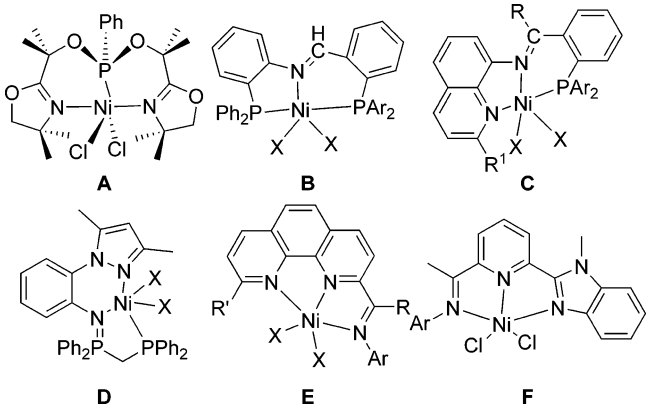

Nickel complexes containing bidentate ligands have been extensively studied in our group. With the **E** model catalyst, the nickel complexes incorporating an additional imino group (R′) unusually showed even better activities than those with their iron and cobalt analogues;[11b] however, the tridentate nickel complexes showed high catalytic activity toward ethylene oligomerization up to the order of 10^7 g mol^{-1}(Ni) h^{-1}.[11f] The coordination environments of all these well-defined catalysts can be systematically varied by changing the substituents of the ligand backbones, which provides an opportunity to control their catalytic behaviors including activity and product distribution. Encouraged by these results, alternative models of tridentate nickel complexes were explored for their catalytic behaviors toward ethylene reactivity, and the metal complexes (**F**) ligated by 2-(1-methyl-2-benzimidazole)-6-(1-aryliminoethyl)pyridines showed high catalytic activity,[12] and good activity was obtained by complexes bearing 2-quinoxalinyl-6-iminopyridines.[13] Challenged by the success of our recently reported N^N^N tridentate nickel complexes, we expect that successive exploration of nickel catalysts, keeping a similar coordination environment and the conjugated electronic system, can further improve catalytic activity and product distribution. Therefore, it would be interesting to substitute the ligand backbone with *N*-((pyridin-2-yl)methylene)quinolin-8-amine derivatives.

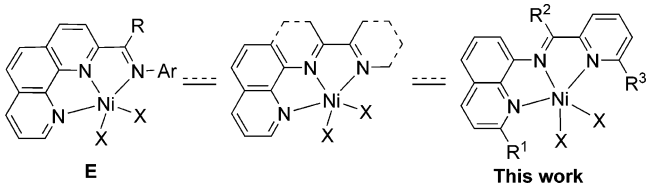

Moreover, during our research toward new tridentate nickel complexes for ethylene oligomerization we often observed a very distinct increase in activity in the previously described system, under the influence of Ph_3P during the oligomerization.[5g,7h,11f,12a,13a] Although the influence of different ancillary phosphines was studied in a ruthenium-based metathesis catalyst[18] and SHOP-type catalysts,[4h] it is still unclear about the influence of different R_3P on the catalytic behavior of tridentate nickel systems. Therefore, the correlations between catalytic activities with various R_3P were investigated in the present paper.

The preparation of *N*-((pyridin-2-yl)methylene)quinolin-8-amine derivatives, however, was not successful due to their instability. Fortunately, we could use a one-pot reaction to synthesize the herein reported nickel complexes. The resultant nickel complexes showed good to high activities up to 4.9×10^7 g mol^{-1}(Ni) h^{-1} for ethylene oligomerization when activated by Et_2AlCl. All these nickel complexes have been carefully characterized along with their unambiguous molecular structures and confirmed by single-crystal X-ray crystallographic analysis. In the following, we report the synthesis and characterization of the nickel complexes along with their catalytic properties for ethylene oligomerization.

2. Results and Discussions

2.1. Synthesis and Characterization of the Complexes. The *N*-((pyridin-2-yl)methylene)quinolin-8-amine derivatives can be formed from the condensation reaction of 8-aminoquinolines with the corresponding pyridine ketones or aldehydes. To introduce bulky substituents such as *i*-Pr, *t*-Bu, and Cy to the framework of the ligand, the substituted 8-nitroquinoline derivatives were synthesized according to literature procedures[14a,b] and

(7) (a) Killian, C. M.; Johnson, L. K.; Brookhart, M. *Organometallics* **1997**, *16*, 2005−2007. (b) Svejda, S. A.; Brookhart, M. *Organometallics* **1999**, *18*, 65−74. (c) Laine, T. V.; Lappalainen, K.; Liimatta, J.; Aitola, E.; Löfgren, B.; Leskelä, M. *Macromol. Rapid Commun.* **1999**, *20*, 487−491. (d) Laine, T.V.; Piironen, U.; Lappalainen, K.; Klinga, M.; Aitola, E.; Leskelä, M. *J. Organomet. Chem.* **2000**, *606*, 112−124. (e) Li, Z.; Sun, W.-H.; Ma, Z.; Hu, Y.; Shao, C. *Chin. Chem. Let.* **2001**, *12*, 691−692. (f) Lee, B. Y.; Bu, X.; Bazan, G. C. *Organometallics* **2001**, *20*, 5425−5431. (g) Shao, C.; Sun, W.-H.; Li, Z.; Hu, Y.; Han, L. *Catal. Commun.* **2002**, *3*, 405−410. (h) Tang, X.; Sun, W.-H.; Gao, T.; Hou, J.; Chen, J.; Chen, W. *J. Organomet. Chem.* **2005**, *690*, 1570−1580. (i) Jie, S.; Zhang, D.; Zhang, T.; Sun, W.-H.; Chen, J.; Ren, Q.; Liu, D.; Zheng, G.; Chen, W. *J. Organomet. Chem.* **2005**, *690*, 1739−1749. (j) Nelkenbaum, E.; Kapon, M.; Eisen, M. S. *J. Organomet. Chem.* **2005**, *690*, 2297−2305. (k) Benito, J. M.; de Jesús, E.; de la Mata, F. J.; Flores, J. C.; Gómez, F.; Gómez-Sal, P. *Organometallics* **2006**, *25*, 3876−3887. (l) Song, C.-L, Tang, L.-M.; Li, Y.-G.; Li, X.-F.; Chen, J.; Li, Y.-S. *J. Polym. Sci., Part A: Polym. Chem.* **2006**, *44*, 1964−1974.

(8) Yang, Q.-Z.; Kermagoret, A.; Agostinho, M.; Siri, O.; Braunstein, P. *Organometallics* **2006**, *25*, 5518−5527.

(9) Speiser, F.; Braunstein, P.; Saussine, L. *J. Chem. Soc., Dalton Trans.* **2004**, 1539−1545.

(10) (a) Hou, J.; Sun, W.-H.; Zhang, S.; Ma, H.; Deng, Y.; Lu, X. *Organometallics* **2006**, *25*, 236−244. (b) Zhang, C.; Sun, W.-H.; Wang, Z.-X.; *Eur. J. Inorg. Chem.* **2006**, *23*, 4895−4902.

(11) (a) Al-Benna, S.; Sarsfield, M. J.; Thornton-Pett, M.; Ormsby, D. L.; Maddox, P. J.; Brès, P.; Bochmann, M. *J. Chem. Soc., Dalton Trans.* **2000**, 4247−4257. (b) Wang, L.; Sun, W.-H.; Han L.; Yang, H.; Hu, Y.; Jin, X. *J. Organomet. Chem.* **2002**, *658*, 62−70. (c) Kunrath, F. A.; De Souza, R. F.; Casagrande, O. L., Jr.; Brooks, N. R.; Young, V. G., Jr. *Organometallics* **2003**, *22*, 4739−4743. (d) Ajellal, N.; Kuhn, M. C. A.; Boff, A. D. G.; Hörner, M.; Thomas, C. M.; Carpentier, J.-F.; Casagrande, O. L., Jr. *Organometallics* **2006**, *25*, 1213−1216. (e) Sun, W.-H.; Jie, S.; Zhang, S.; Zhang, W.; Song, Y.; Ma, H.; Chen, J.; Wedeking, K.; Fröhlich, R. *Organometallics* **2006**, *25*, 666−677. (f) Sun, W.-H.; Zhang, S.; Jie, S.; Zhang, W.; Li, Y.; Ma, H.; Chen, J.; Wedeking, K.; Fröhlich, R. *J. Organomet. Chem.* **2006**, *691*, 4196−4203. (g) Jie, S.; Zhang, S.; Sun, W.-H.; Kuang, X.; Liu, T.; Guo, J. *J. Mol. Catal. A: Chem*. **2007**, *269*, 85−96. (h) Zhang, M.; Zhang, S.; Hao, P.; Jie, S.; Sun, W.-H.; Li, P.; Lu, X. *Eur. J. Inorg. Chem.* **2007**, 3816−3826.

(12) (a) Hao, P.; Zhang, S.; Sun, W.-H.; Shi, Q.; Adewuyi, S.; Lu, X.; Li, P. *Organometallics* **2007**, *26*, 2439−2446. (b) Sun, W.-H.; Hao, P.; Zhang, S.; Shi, Q.; Zuo, W.; Tang, X.; Lu, X. *Organometallics* **2007**, *26*, 2720−2734.

(13) (a) Adewuyi, S.; Li, G.; Zhang, S.; Wang, W.; Hao, P.; Sun, W.-H.; Tang, N.; Yi, J. *J. Organomet. Chem.* **2007**, *692*, 3532−3541. (b) Sun, W.-H.; Hao, P.; Li, G.; Zhang, S.; Wang, W.; Yi, J.; Asma, M.; Tang, N. *J. Organomet. Chem.* **2007** (DOI: 10.1016/j.jorganchem.2007.04.027).

(14) (a) Vangapandu, S.; Jain, M.; Jain, R.; Kaur, S.; Singh, P. P. *Bioorg. Med. Chem.* **2004**, *12*, 2501−2508. (b) Jordis, U.; Sauter, F.; Rudolf, M.; Cai, G. *Monatsh. Chem.* **1988**, *119*, 761−780. (c) Riesgo, E. C.; Jin, X.; Thummel, R. P. *J. Org. Chem.* **1996**, *61*, 3017−3022.

(15) Lions, F.; Martin, K. V. *J. Am. Chem. Soc.* **1957**, *79*, 2733−2738.

(16) (a) Esteruelas, M. A.; López, A. M.; Méndez, L.; Oliván, M.; Oñate, E. *Organometallics* **2003**, *22*, 395−406. (b) Gasperini, M.; Ragaini, F.; Cenini, S. *Organometallics* **2002**, *21*, 2950−2957.

(17) Butchler, R. J.; Sinn, E. *Inorg. Chem.* **1977**, *16*, 2334−2343.

(18) Love, J. A.; Sanford, M. S.; Day, M. W.; Grubbs, R. H. *J. Am. Chem. Soc*. **2003**, *125*, 10103−10109.

Scheme 2. Synthesis of Tridentate Nickel Complexes

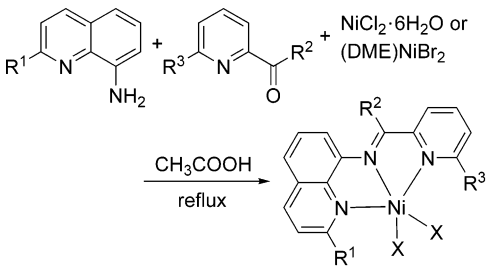

	1a	2a	3a	4a	5a	6a	7a	8a	9a	10a	11a	12a
R^1	H	Me	H	Me	*i*-Pr	*i*-Pr	*t*-Bu	*t*-Bu	Cy	Cy	H	H
R^2	H	H	H	H	H	H	H	H	H	H	Me	Ph
R^3	H	H	Me	Me	H	Me	H	Me	H	Me	H	H
X	Cl	Cl	Cl	Cl	Cl	Cl	Cl	Cl	Cl	Cl	Cl	Cl

	1b	2b	3b	4b	5b	6b	7b	8b	9b	10b	11b	12b
R^1	H	Me	H	Me	*i*-Pr	*i*-Pr	*t*-Bu	*t*-Bu	Cy	Cy	H	H
R^2	H	H	H	H	H	H	H	H	H	H	Me	Ph
R^3	H	H	Me	Me	H	Me	H	Me	H	Me	H	H
X	Br	Br	Br	Br	Br	Br	Br	Br	Br	Br	Br	Br

then reduced by iron powder in acidic solution to form 8-aminoquinolines.[14c] All 8-nitroquinoline and 8-aminoquinoline derivatives were confirmed by NMR spectroscopy.[14a]

A typical Schiff-base reaction was carried out by reacting 8-aminoquinolines with the corresponding pyridine ketones or aldehydes, leading to the preparation of *N*-((pyridin-2-yl)-methylene)quinolin-8-amine derivatives. Much effort was spent isolating the Schiff-base compounds; however, these compounds tend to decompose when separated by column chromatography, and pure products could not be obtained.[15] As generally applied to either unstable or low-yielding ligands, the one-pot synthesis technique was therefore employed to prepare the metal complexes in good yields.[7l,10a,16] The central cationic nickel was introduced *in situ* along with the condensation reaction of pyridine-2-aldehyde or ketone and 8-aminoquinolines. Stoichiometric amounts of the 8-aminoquinoline derivative, pyridine-2-aldehyde, or ketone and the nickel dihalides were mixed and refluxed in acetic acid for 4 h to afford the corresponding complexes (Scheme 2). The resulting products were precipitated from the reaction solution, collected by filtration, washed with diethyl ether, and dried under vacuum. The complexes were separated as air-stable powders in moderate to high yields. All complexes were characterized by elemental analysis and IR spectroscopy. The IR spectra of complexes **1a**−**12a** and **1b**−**12b** show a strong and sharp band in the range 1595−1630 cm^{-1} that can be ascribed to the stretching vibration of C═N; however, their elemental analysis revealed that some of them contained water or solvent in their solid state. The NMR data were not obtained due to the paramagnetic nature of these nickel complexes. Their unambigious molecular structures were confirmed by single-crystal X-ray crystallography.

2.2. Crystal Structures. X-ray crystallographic analyses revealed that these nickel complexes could form either dimeric or monomeric structures in the solid state. Using various substituents of the same framework, nickel complexes with monomeric and dimeric structures were reported a long time ago for a bidentate N^N system.[17] In that case, dimeric structures were observed for the chlorides, while both dimeric and monomeric structures were observed for the bromides. These results point out that steric and electronic effects of the ligands play important roles in forming solid-state structures of the complexes. The catalytic properties of nickel complexes have been considered as a driving force in this work, but interestingly their molecular structures show some unique properties of coordination. Therefore, some discussions on their molecular structures are useful in coordination chemistry.

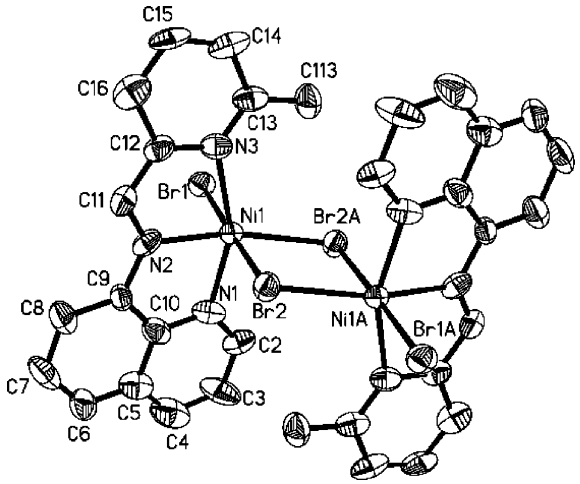

Figure 1. Molecular structure of **3b**, with thermal ellipsoids at the 30% probability level. Hydrogen atoms and solvent are omitted for clarity.

Fortunately, crystal structures of some of the complexes (**3b**, **4a**, **6a**, **6b**, **10a**, **10b**, **11a**, and **12a**) aided the understanding of the driving force for the formation of monomeric and dimeric structures. When the steric demand of R^1 and R^3 is minor, the molecular geometry prefers to build up an octahedral-coordinated type. This coordination can be realized through the formation of dimers, using bridged halogen atoms (**3b**, **12a**) or an additional solvent coordination to the metal (**11a**). Complexes bearing bulkier substituents R^1 and R^3 display a distorted trigonal-bipyramidal geometry; this is realized through a monomeric structure, in which the nickel is coordinated by the tridentate ligand and two halides (**4a**, **6a**, **6b**, **10a**, and **10b**).

Crystals of **3b**, showing a dimeric structure in the solid state, were grown from a methanol solution through slow evaporation of the solvent at room temperature. The molecular structure is shown in Figure 1, and selected bond lengths and angles are listed in Table 1. The coordination of the nickel centers can be described as distorted octahedron geometry. Each nickel atom is coordinated by three N atoms (N(1), N(2), and N(3)) of the ligand, one terminal bromide (Br(1)), and two bridging bromides (Br(2) and Br(2A)). The N(2)−C(11) bond distance is 1.24(2) Å, which is in accordance with a C═N bond, confirming the formation of a Schiff base in the one-pot method employed. The distance between the nickel and the terminal bromide (Ni(1)−Br(1)) is 2.533(2) Å, whereas, the bond lengths between the nickel and the two bridging bromides differ significantly (2.505(2) and 2.638(2) Å). The bridge is planar, leading to a Ni(1)−Ni(1A) distance of 3.811 Å, suggesting that there is no direct metal−metal interaction. Each nickel forms two five-membered chelate rings with three nitrogen atoms; the bite angles of N(2)−Ni(1)−N(1) and N(2)−Ni(1)−N(3) are 79.1-(5)° and 77.2(5)°, respectively. The Ni(1) atom deviates by 0.044 Å from the plane of the Br(1)−N(2)−Br(2) atoms and deviates by 0.066 Å from the plane of the N(1)−N(2)−N(3) atoms. The plane of Br(1)−N(2)−Br(2) lies almost perpendicular to the plane formed by N(1)−Ni(1)−N(3) with the dihedral angle of 87.9°, and the quinoline plane is nearly coplanar with the

Table 1. Selected Bond Lengths (Å) and Angles (deg) for the Dimeric Complex 3b

	3b (X = Br)
Bond Lengths	
Ni(1)−N(1)	2.08(2)
Ni(1)−N(2)	2.02(2)
Ni(1)−N(3)	2.22(2)
N(2)−C(11)	1.24(2)
Ni(1)−Br(1)	2.533(2)
Ni(1)−Br(2)	2.638(2)
Ni(1)−Br(2)#1	2.505(2)
Bond Angles	
N(2)−Ni(1)−N(1)	79.1(5)
N(2)−Ni(1)−N(3)	77.2(5)
N(1)−Ni(1)−N(3)	156.1(5)
N(2)−Ni(1)−Br(2)#1	166.4(3)
N(2)−Ni(1)−Br(2)	84.4(3)
N(1)−Ni(1)−Br(2)#1	93.3(4)
N(1)−Ni(1)−Br(2)	90.7(4)
N(3)−Ni(1)−Br(2)#1	110.5(3)
N(3)−Ni(1)−Br(2)	89.7(3)
Br(2)#1−Ni(1)−Br(1)	95.88(7)
Br(1)−Ni(1)−Br(2)	178.05(8)
N(1)−Ni(1)−Br(1)	91.2(4)
N(2)−Ni(1)−Br(1)	95.6(3)
N(3)−Ni(1)−Br(1)	88.4(3)
Br(2)#1−Ni(1)−Br(2)	84.40(7)
Ni(1)#1−Br(2)−Br(1)	95.60(7)

pyridine ring, the dihedral angle being 4.3°. In addition, complex **12a** ($R^1 = R^3 = H$; $R^2 = Ph$) shows the same structural features as **3b**.

Complex **11a** demonstrates another way to form distorted octahedral coordination geometry around the Ni center. Crystals of **11a** were obtained from a methanol solution through slow evaporation of the solvent. The molecular structure is shown in Figure 2, and selected bond lengths and angles are listed in Table 2. The octahedral geometry around the nickel is formed by three N atoms of the ligand, two O atoms of coordinated methanol solvent, and one Cl atom, which is clearly different from the observed case in **3b**. The other Cl atom is displaced from its coordinated state and found separated as Cl^-. The Ni atom deviates 0.076 Å out of the O(100)−N(2)−O(200) plane and deviates 0.010 Å out of the N(1)−N(2)−N(3) plane. The dihedral angle between the quinoline plane and the pyridine plane is measured to be 8.4°. The dihedral angle between O(100)−N(2)−O(200) and the N(1)−Ni(1)−N(3) plane is 89.0°.

Crystals of **4a** suitable for X-ray structural determination were grown from a methanol solution through slow evaporation of

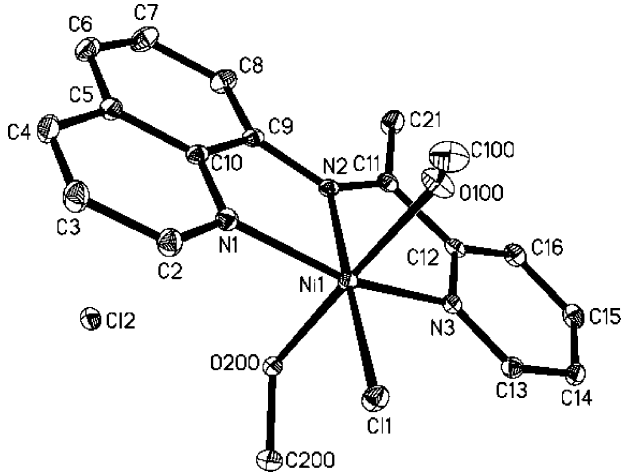

Figure 2. Molecular structure of **11a**. Thermal ellipsoids are drawn at the 30% probability level. Hydrogen atoms are omitted for clarity.

Table 2. Selected Bond Lengths (Å) and Angles (deg) for Complex 11a

Bond Lengths			
Ni(1)−N(1)	2.046(2)	Ni(1)−O(100)	2.124(2)
Ni(1)−N(2)	2.066(2)	Ni(1)−Cl(1)	2.346(2)
Ni(1)−N(3)	2.049(2)	N(2)−C(11)	1.291(3)
Ni(1)−O(200)	2.117(2)		
Bond Angles			
N(1)−Ni(1)−N(2)	80.27(8)	N(3)−Ni(1)−O(100)	87.05(8)
N(1)−Ni(1)−N(3)	159.04(8)	O(200)−Ni(1)−O(100)	174.69(7)
N(3)−Ni(1)−N(2)	78.77(8)	N(1)−Ni(1)−Cl(1)	100.04(6)
N(1)−Ni(1)−O(200)	90.23(8)	N(2)−Ni(1)−Cl(1)	178.77(6)
N(2)−Ni(1)−O(200)	87.34(7)	N(3)−Ni(1)−Cl(1)	100.92(6)
N(3)−Ni(1)−O(200)	88.34(8)	N(3)−Ni(1)−Cl(1)	88.4(3)
N(1)−Ni(1)−O(100)	93.12(8)	O(200)−Ni(1)−Cl(1)	93.84(5)
N(2)−Ni(1)−O(100)	89.17(7)	O(100)−Ni(1)−Cl(1)	89.63(5)

Table 3. Selected Bond Lengths (Å) and Angles (deg) for the Monomeric Complexes 4a, 6a, and 10a

	4a (X = Cl)	**6a** (X = Cl)	**10a** (X = Cl)
Bond Lengths			
Ni(1)−N(1)	2.112(4)	2.147(3)	2.100(3)
Ni(1)−N(2)	1.980(4)	2.000(2)	1.990(3)
Ni(1)−N(3)	2.140(4)	2.167(3)	2.128(3)
Ni(1)−Cl(1)	2.274(2)	2.279(2)	2.289(2)
Ni(1)−Cl(2)	2.295(2)	2.284(2)	2.294(2)
N(2)−C(11)	1.272(5)	1.279(4)	1.272(5)
Bond Angles			
N(2)−Ni(1)−N(1)	79.7(2)	79.02(9)	80.0(2)
N(2)−Ni(1)−N(3)	78.5(2)	78.36(9)	79.0(2)
N(1)−Ni(1)−N(3)	158.0(2)	157.4(1)	159.0(2)
N(1)−Ni(1)−Cl(1)	94.7(2)	93.61(7)	94.41(9)
N(2)−Ni(1)−Cl(1)	110.4(2)	110.58(8)	110.9(1)
N(3)−Ni(1)−Cl(1)	95.3(2)	93.65(7)	92.5(1)
N(1)−Ni(1)−Cl(2)	95.2(2)	96.39(7)	93.7(1)
N(2)−Ni(1)−Cl(2)	113.2(2)	118.26(8)	110.4(1)
N(3)−Ni(1)−Cl(2)	91.0(2)	94.89(7)	94.2(1)
Cl(1)−Ni(1)−Cl(2)	136.38(6)	131.15(4)	138.69(5)

the solvent, whereas crystals of **6a**, **6b**, **10a**, and **10b** were grown from a slow diffusion of diethyl ether into a methanol solution of the corresponding complex. Related bond lengths and angles of these comparable complexes are shown in Table 3.

When the steric bulk of the substituents R^1 and R^3 is increased, these complexes form monomeric structures. X-ray analysis reveals that each nickel atom is coordinated with three N atoms (N(1), N(2), and N(3)) of the ligand and two halogens. The geometry around the nickel atom displays a distorted trigonal bipyramid in which an equatorial plane is formed by the imine nitrogen (N(2)) and the two halogens, while the nitrogen (N(1)) of the quinolyl group and the nitrogen (N(3)) of the pyridyl group are located in axial positions. For these five monomeric structures, two features in common could be observed. One is that the distances between nickel and coordinated nitrogens have the same trend: Ni(1)−N(3) > Ni(1)−N(1) > Ni(1)−N(2); the other is that the angles N(1)−Ni(1)−N(2) and N(2)−Ni(1)−N(3) are hardly effected by the halogen and R^1 substituents.

The molecular structure of **4a** is shown in Figure 3. Although the Me substituent in complex **4a** is not very bulky, a monomeric structure could also be observed. The N(2)−C(11) bond distance is 1.272(5) Å, displaying clear C═N double-bond character. The Ni−N bonds are different from each other. The shortest bond, at 1.980(4) Å, is found for the imine-N (Ni(1)−N(2)), followed by the quinoline-N with a Ni(1)−N(1) of 2.112(4) Å and the pyridine-N with a Ni(1)−N(3) of 2.140 Å. This trend is observed for all following monomeric structures. The Ni center deviates by 0.032 Å out of the equatorial plane. The axial plane is almost vertical to the equatorial plane, with a dihedral angle of 88.6°. Like the previously discussed structures, the ligand backbone

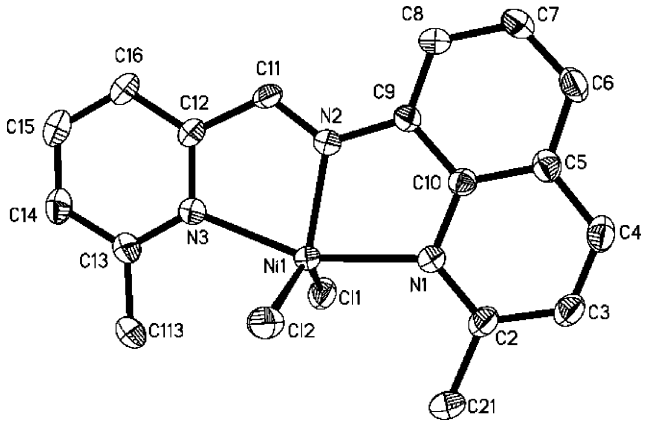

Figure 3. Molecular structure of **4a**, with thermal ellipsoids at the 30% probability level. Hydrogen atoms and solvent are omitted for clarity.

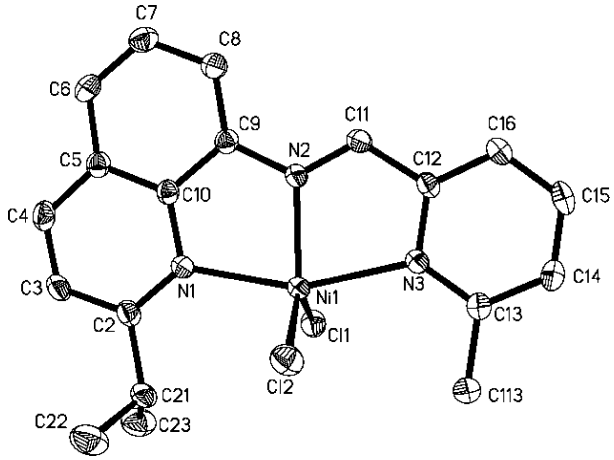

Figure 4. Molecular structure of **6a**, with thermal ellipsoids at the 30% probability level. Hydrogen atoms are omitted for clarity.

of **4a** is not planar, having a dihedral angle of 7.3° between quinoline and the pyridine ring.

The molecular structure of **6a** is displayed in Figure 4. Comparing bond lengths and angles of these complexes (Table 3 and Supporting Information), the influence of the halide seems to be rather minimal. The Ni−N bonds show the same trend as observed for **4a**, and *i*-Pr makes the Ni−N(1) bond slightly longer than **4a**. The angle between the two axially positioned N atoms (N(1)−Ni(1)−N(3)) shows only a small deviation (157.4(1)°). The axial plane is almost vertical to the equatorial plane, with the dihedral angle of 90.4°. The dihedral angle measured between the pyridine and the quinoline is 3.6°. Its bromide analogue **6b** was also determined with single-crystal X-ray analysis and showed the same structural features as **6a**.

The molecular structure of **10a** is displayed in Figure 5. With further increase in the steric bulk of the substituent at the R^1 position the same trend in bond lengths and angles can be observed as in **4a** and **6a** (Table 3). For **10a**, however, the Ni−N(1) bond is even shorter than **4a**, and a chair conformation could be observed for the cyclohexyl group. The ligand is not perfectly coplanar, with a dihedral angle between the pyridine and the quinoline ring of 2.5°. The Ni atoms deviate slightly out of the equatorial plane spanned by X(1)−N(2)−X(2) (0.015 Å, **10a**). The axial plane is almost vertical to the equatorial plane, with a dihedral angle of 89.4°. The single-crystal X-ray analysis revealed that **10b** has the same structural features as its analogue **6a**.

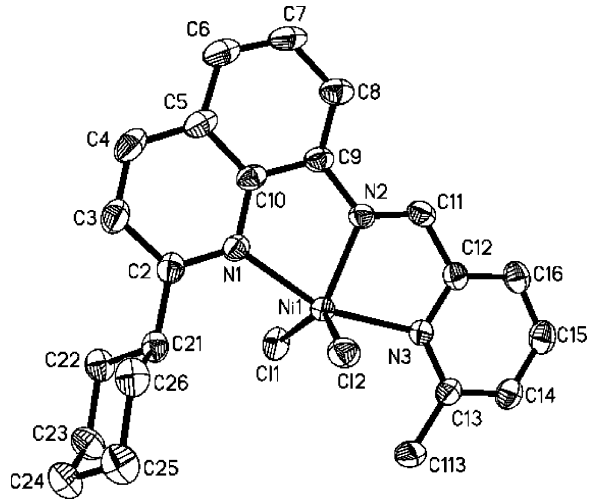

Figure 5. Molecular structure of **10a**, with thermal ellipsoids at the 30% probability level. Hydrogen atoms and solvent are omitted for clarity.

Table 4. Oligomerization of Ethylene with 6a/Et_2AlCl[a]

entry	Al/Ni	*T* (°C)	*P* (atm)	oligomer distribution(%) C_4	α-C_4	C_6	activity (10^5 g mol^{-1}(Ni) h^{-1})
1	200	20	30	96.9	96.2	3.1	8.3
2	500	20	30	92.9	91.2	7.1	33.9
3	700	20	30	96.7	93.4	3.3	14.0
4	1000	20	30	97.9	54.9	2.1	9.2
5	500	20	10	96.8	87.6	3.2	3.7
6	500	20	20	95.0	94.1	5.0	17.6
7	500	40	30	94.9	91.2	5.1	15.6
8	500	60	30	93.3	92.3	6.7	12.7
9	500	80	30	97.9	80.0	2.1	6.8

[a] General conditions: 5 μmol of complex; 100 mL of toluene; 20 min.

2.3. Ethylene Oligomerization. The nickel(II) complexes **1a**−**12a** and **1b**−**12b** were systematically investigated for ethylene oligomerization. Various aluminum activators were scanned as cocatalysts to activate the title nickel complexes for ethylene reactivity. The best results were obtained using diethylaluminum chloride (Et_2AlCl) as cocatalyst with catalytic activities on the order of 10^5−10^6 g mol^{-1}(Ni) h^{-1}. Therefore, Et_2AlCl was used as an activator for further investigations. Dimerization with moderate to high selectivity for α-C_4 dominates along with minor amounts of trimers. Compared with a typical catalyst $(Cy_3P)_2NiCl_2$[3d] for ethylene dimerization, the current catalytic systems herein showed much higher selectivity for α-C_4. There were several isomers of hexenes detected with low content of 1-hexene (<15%). Because of the low amount of C_6 (<10% of total oligomers), the individual isomers of hexenes could not be quantified accurately. According to the mechanism proposed by Braunstein,[8] the formation of various hexenes could be inferred by reincorporation of butene.

2.3.1. Effects of Reaction Parameters on Catalytic Behavior. Considering the ethylene reactivity, the reaction parameters including the ratio of Et_2AlCl to nickel complex, pressure of ethylene, and reaction temperature affect the catalytic activities. The influence of different reaction parameters on ethylene oligomerization was investigated in detail with complexes **6a** and **1b**. The oligomerization results using complexes **6a** and **1b** are summarized in Tables 4 and 5, respectively. As revealed in Tables 4 and 5, the reaction parameters significantly affect the catalytic activity; however, no obvious influence on the product distribution could be observed.

With complex **6a**, the amount of Et_2AlCl played an important role in the catalytic properties. Increasing the Al/Ni molar ratio

Table 5. Oligomerization of Ethylene with 1b/Et_2AlCl[a]

entry	Al/Ni	*T* (°C)	*P* (atm)	oligomer distribution (%) C_4	α-C_4	C_6	activity (10^5 g mol^{-1}(Ni) h^{-1})
1	200	20	30	96.9	90.5	3.1	16.0
2	500	20	30	95.9	93.8	4.1	47.2
3	700	20	30	96.3	70.9	3.7	23.5
4	1000	20	30	95.6	84.5	4.4	15.4
5	500	20	10	95.8	90.3	4.2	6.6
6	500	20	20	95.2	72.1	4.8	30.1
7	500	40	30	93.4	86.7	6.6	25.7
8	500	60	30	92.7	69.1	7.3	19.1
9	500	80	30	92.9	64.1	7.1	6.9

[a] General conditions: 5 μmol of complex; 100 mL of toluene; 20 min; Et_2AlCl.

from 200 to 500 (entries 1 and 2 in Table 4), the highest activity (33.9×10^5 g mol^{-1}(Ni) h^{-1}, entry 2 in Table 4) was observed at an Al/Ni ratio of 500. However, when the Al/Ni molar ratio was further increased (entries 2−4 in Table 4), the activity decreased.

Ethylene oligomerization of complex **6a** was also carried out at different pressures (entries 1, 5, and 6 in Table 4). As expected, the catalytic activities predominantly decreased at lower ethylene pressure, due to lower monomer concentration at lower pressure.

The reaction temperature significantly affects the catalytic activity. Elevation of the temperature from 20 °C to 80 °C (entries 2 and 7−9 in Table 4) led to a significant decline in activity, probably due to the decomposition of the catalysts and lower ethylene solubility at higher temperature.

A similar influence was also observed with complex **1b**. Different reaction temperature, amount of cocatalyst, and pressure of ethylene also affected its catalytic reactivity. The Al/Ni molar ratio was varied from 200 to 1000. However, the optimum Al/Ni molar ratio for ethylene oligomerization was fixed at 500. Elevating the reaction temperature from 20 °C to 80 °C resulted in decreased catalytic activity, and lower catalytic activity was observed at lower pressure.

2.3.2. Effect of the Ligand Environment on the Catalytic Behavior. Complexes **1a**−**12a** and **1b**−**12b** were examined for oligomerization of ethylene at 30 atm, and the results are summarized in Table 6. The substitution pattern of the ligand plays a major role in the performance of the catalysts.

The effect of the substitution pattern of the R^2 substituent on the imino-C of the ligands is significant. Varying the electron-donating properties of R^2 (entries 1, 11, 12, X = Cl, and 13, 23, 24, X = Br, in Table 6), the highest activities were observed when R^2 = H (entries 1 and 13 in Table 6). However, with R^2 = Me, (entries 11 and 23 in Table 6) the observed activities decreased. On changing R^2 to a stronger electron-donating phenyl group (entries 12 and 24 in Table 6), the activity further decreased.

The substituents R^1 and R^3 have considerable effects on the catalytic behaviors. The highest activities of 41.2×10^5 (entry 1 in Table 6) and 47.2×10^5 g mol^{-1}(Ni) h^{-1} (entry 13 in Table 6) were obtained with the least bulky complexes **1a** and **1b**. However, increasing the steric bulk (complexes **2a** to **4a**, **2b** to **4b**) at the Me substituent resulted in a decreased activity (entries 2−4 and 14−16 in Table 6). A possible explanation is that the active site of the catalyst is blocked through bulky substituents, leading to a decline in activities.

Furthermore, on changing the R^1 substituent from Me to *i*-Pr, *t*-Bu, or Cy while keeping R^3 = Me (entries 4, 6, 8, and 10 and 16, 18, 20, and 22 in Table 6), higher activities were observed. A possible explanation could be found in two opposing effects. One is that the active site of the catalyst is blocked through bulky substituents, leading to a decline in activity, while on the other hand, these bulky substituents are protecting the active center against decomposition, affording higher activities. Hence, the overall effect depends on the type of substituent.

Table 6. Ethylene Oligomerization with 1a−12a and 1b−12b/Et_2AlCl[a]

entry	cat.	oligomer distribution (%) C_4	α-C_4	C_6	activity (10^5 g mol^{-1}(Ni) h^{-1})
1	**1a**	97.5	82.4	2.5	41.2
2	**2a**	98.6	92.9	1.4	20.3
3	**3a**	96.2	89.4	3.8	6.8
4	**4a**	98.3	85.6	1.7	7.7
5	**5a**	96.3	91.4	3.7	19.2
6	**6a**	92.9	91.2	7.1	33.9
7	**7a**	96.4	83.3	3.6	9.2
8	**8a**	98.0	94.4	2.0	20.1
9	**9a**	97.9	88.5	2.1	5.0
10	**10a**	95.9	94.1	4.1	14.1
11	**11a**	95.2	83.7	4.8	21.4
12	**12a**	94.8	89.2	5.2	10.7
13	**1b**	96.7	93.8	3.3	47.2
14	**2b**	95.2	89.6	4.8	26.6
15	**3b**	97.6	91.8	2.4	15.2
16	**4b**	96.5	88.0	3.5	13.7
17	**5b**	94.8	92.4	5.2	22.1
18	**6b**	96.8	91.9	3.2	21.9
19	**7b**	96.3	91.1	3.7	25.8
20	**8b**	96.6	91.7	3.4	22.9
21	**9b**	95.2	92.9	4.8	15.1
22	**10b**	96.3	90.6	3.7	13.8
23	**11b**	97.7	92.7	2.3	35.0
24	**12b**	96.6	94.8	3.4	18.5

[a] General conditions: 5 μmol of complex; 100 mL of toluene; 20 min; 20 °C; Et_2AlCl, Al/Ni = 500; 30 atm.

As to the product distribution, it is surprising to observe that the substituents have a minimal influence. In the total amount of olefins formed in the oligomerization reactions, C_4 content varied from 92.9% (entry 6 in Table 6) to 98.6% (entry 2 in Table 6) when different complexes were evaluated under identical reaction conditions. For other tridentate N^N^N Ni complexes, similar results had been observed before.[11d,f,12a]

The influence of the halide anion linked to the nickel center could be evaluated by comparing entries 1 to 12 with 13 to 24. In most cases, the dibromonickel complex shows higher activity than their dichloronickel analogue, and it could be explained by the better solubility of the bromo compound than the chloro analogue.

2.3.3. Effects of R_3P as Auxiliary Ligand on the Catalytic Behavior. For a long time the influence of the auxiliary phosphine ligand in SHOP-type catalysts on activity and selectivity was believed to be minor. The phosphine was thought to be necessary only to stabilize the nickel center.[4a] In fact, phosphine ligands play an important role in different catalytic systems. One of the initiating steps in the oligomerization of ethylene catalyzed by SHOP-type catalysts is the generation of the active species via the dissociation of the phosphine ligand from the hydride species, forming an unstable 14 e^- species that acts as the active species for ethylene oligomerization. Chain growth can occur via coordination and insertion of ethylene. The Braunstein group systematically investigated the effect of different phosphines on the catalytic activity of the SHOP catalyst, and similar observations concerning the influence on the generation of the active species were made.[4b] The nature of the phosphine mainly influences activity and length of the resulting oligomers. Weakly coordinating phosphines such as Ph_3P and Tol_3P produce higher molecular weight oligomers, whereas catalysts containing strongly coordinating phosphines

Table 7. Oligomerization of Ethylene with R_3P[a]

entry	cat.	R_3P	t (min)	oligomer distribution (%) C_4	α-C_4	C_6	activity (10^7 g mol^{-1}(Ni) h^{-1})
1	**1a**	Ph_3P	20	91.3	20.5	8.7	2.9
2	**1b**	Ph_3P	20	90.2	13.8	9.8	2.5
3	**10a**	Ph_3P	20	91.2	18.4	8.8	2.3
4	**12a**	Ph_3P	20	93.3	17.1	6.7	3.1
5	**1a**	Cy_3P	20	86.5	86.2	13.5	4.9
6	**1b**	Cy_3P	20	91.7	75.9	8.3	4.7
7	**1b**	Cy_3P	60	95.4	34.6	4.6	2.2
8	**1a**	$(C_6F_5)_3P$	20	95.5	82.4	4.5	0.2
9	**1b**	$(C_6F_5)_3P$	20	94.1	85.8	5.9	0.1

[a] General conditions: 5 μmol of complex; 100 mL of toluene; 20 °C; Et_2AlCl, Al/Ni = 500; 30 atm; 25 equiv of R_3P.

such as Me_3P and $PhMe_2P$ produce low molecular weight oligomers with significantly lower activities. By using phosphine scavengers such as $Ni(COD)_2$ even the production of polyethylene is possible. In the mechanism proposed by Braunstein, recoordination of phosphine leads to chain termination via β-hydride elimination and re-formation of the initial 16 e$^-$ hydride species.[4b] Matt and Monteiro recently suggested that a second termination mechanism is likely to occur.[4f] Matt proposed a five-coordinated 18 e$^-$ ethylene/R_3P intermediate that undergoes chain termination via β-hydrogen transfer to the coordinated olefin. Carlini reported a bis(salicylaldiminate)-nickel(II) system that in the presence of MAO and auxiliary phosphines shows higher activities for ethylene oligomerization compared to the phosphine-free system, whereas the product distribution turns to lower oligomers and the selectivity for α-olefin decreases.[5c] However, to the best of our knowledge, the influence of different R_3P as auxiliary ligands on tridentate nickel systems has not been reported. To get a better understanding of the actual influence, in our system the following phosphines have been used: Cy_3P, Ph_3P, $(C_6F_5)_3P$, Ph_2MeP, and $PhMe_2P$. These phosphines differ in their electronic properties, as well in their steric properties.

Using 25 equiv of Ph_3P, the activities of the complexes increased significantly, reaching a high activity level of 10^7 g mol^{-1}(Ni) h^{-1}, which is much higher than the catalytic systems without Ph_3P (entries 1−4 in Table 7). For example, with complex **12a** more than 29 times higher activity was observed (3.1×10^7 g mol^{-1}(Ni) h^{-1}). However, the selectivity for α-C_4 decreased sharply. This is consistent with previous reports by other groups[4d,5c] and could be attributed to a higher isomerization rate.

By replacing Ph_3P with PCy_3 even higher activities could be obtained (entries 5−7 in Table 7). For complex **1a**, its activity is as high as 4.9×10^7 g mol^{-1}(Ni) h^{-1}, one of the highest results ever reported. For complex **1b**, a similar trend is also observed here when comparing the data between entry 2 and entry 6, and **1b** still remains active even after 1 h (entry 7 in Table 7). The reason could be attributed to the bulkiness of the Cy group, which results in easy dissociation of the metal−phosphorus bond.[4d,e,g]

The results we got by using electron-deficient $(C_6F_5)_3P$ as ancillary ligands are not what we expected. Due to its electron deficiency, the basicity of $(C_6F_5)_3P$ is low and supposed to result in much higher activities; however, the system hardly exerts an acceleration effect for the oligomerization of ethylene (entries 8 and 9 in Table 7). Perhaps $(C_6F_5)_3P$ contains electron-withdrawing fluoro substituents; it is difficult for $(C_6F_5)_3P$ to donate its electrons to coordinate with the metal center.

To evaluate the influence of basicity of R_3P, a series of phosphines such as Ph_3P, Ph_2MeP, and $PhMe_2P$ were employed in a catalytic reaction at 1 atm, and the results are summarized

Table 8. Oligomerization of Ethylene with the 1b/Et_2AlCl/R_3P System[a]

entry	R_3P	oligomer distribution (%) C_4	α-C_4	C_6	activity (10^4 g mol^{-1}(Ni) h^{-1})
1[b]		100	61.5		6.3
2	Ph_3P	97.3	6.2	2.7	70
3	Ph_2MeP	100	4.4		5.1
4	$PhMe_2P$	100	39.2		1.2

[a] General conditions: 5 μmol of complex; 1 atm; 30 mL of toluene; 20 min; 20 °C; Et_2AlCl, Al/Ni = 500; 25 equiv of R_3P. [b] R_3P was not used.

Table 9. Oligomerization of Ethylene with the 1b/Et_2AlCl/R_3P System[a]

entry	R_3P	t (min)	oligomer distribution (%) C_4	α-C_4	C_6	activity (10^5 g mol^{-1}(Ni) h^{-1})
1	Ph_3P	5	100	37.6	0	3.0
2	Ph_3P	10	98.8	17.1	1.2	9.6
3	Ph_3P	20	97.3	6.2	2.7	7.0
4	Ph_3P	40	95.9	5.4	4.1	5.0
5	Ph_3P	60	94.5	5.0	5.5	3.5
6	Ph_3P	90	94.2	5.0	5.8	2.4
7	Cy_3P	5	95.1	78.5	4.9	6.1
8	Cy_3P	10	90.6	39.8	9.4	9.8
9	Cy_3P	20	88.3	15.9	11.7	10.7
10	Cy_3P	40	87.8	10.6	12.2	7.4
11	Cy_3P	60	86.3	8.4	13.7	5.4
12	Cy_3P	90	85.7	7.1	14.3	3.6

[a] General conditions: 5 μmol of complex; 30 mL of toluene; 20 °C; Et_2AlCl, Al/Ni = 500; 1 atm; 25 equiv of R_3P.

in Table 8. The results we got for Ph_3P, Ph_2MeP, and $PhMe_2P$ are in line with the observations made by Braunstein[4b] and Keim[4d] for the SHOP catalyst and by Grubbs for the metathesis catalyst.[18] It was concluded that the coodination of the phosphine ligand with higher basicity to the metal center becomes so strong that the initiation step, the dissociation of the phosphine, becomes difficult and only small amounts of active species are formed. For our N^N^N nickel system, the declining activities of the complexes were observed with increasing the basicity of their phosphine ligands; Ph_2MeP and $PhMe_2P$ showed less activity compared with a phosphine-free system (entries 1−4 in Table 8), and a stronger binding of the more basic phosphines to the nickel center blocked coordination of ethylene on the active species. Although Cy_3P itself shows a more basic property (pK_a is 9.7), better catalytic activities were obtained (entries 5−7 in Table 7). It could be assumed that the bulkiness of the Cy_3P ligand has a major influence due to the nonplanar ring Cy group and the existing tridentate N^N^N ligand, the combined effect resulting in a relative weak bonding of Cy_3P with the nickel center along with the tendency for stronger bonding of the phosphine to the nickel center. The presence of Cy_3P could stabilize active species and prepare space for ethylene coordination; therefore, the catalytic activities were increased. Similar observations were also obtained by another group.[4g]

Furthermore, the effect of auxiliary ligand on the catalyst lifetime was also investigated. The selectivity and catalyst activity were monitored versus time in the **1b**/Et_2AlCl/Ph_3P and **1b**/Et_2AlCl/Cy_3P systems at 1 atm, and the results are summarized in Table 9. For both cases, activities remained high over a 5−20 min period, indicating a rather long lifetime and good thermal stability of the catalytic species. Moreover, the content of C_6 increased gradually along with reaction time due to plausible reincorporation of 1-butene. However, the selectivity for α-C_4 decreased with time, indicating a high isomerization rate.

3. Conclusions

A series of tridentate (N^N^N) nickel complexes of *N*-((pyridin-2-yl)methylene)quinolin-8-amine derivatives have been synthesized and fully characterized. Due to the instability of the ligands, the complexes were synthesized through a metal-induced template reaction. X-ray crystallographic analysis revealed that these nickel complexes could form dimeric or monomeric structures. It was further confirmed that the substituents, instead of the halides, determine the formation of dimeric or monomeric structures. Upon activation with Et_2AlCl, all nickel complexes exhibited considerably high catalytic activity for ethylene oligomerization with dimers and trimers as products. The selectivity for α-C_4 is moderate to high. Both substituents and catalytic reaction parameters significantly affect the catalytic activity. In the presence of 500 equiv of Et_2AlCl, complex **1b** showed a high activity of 4.7×10^6 g mol^{-1}(Ni) h^{-1}. In addition, the influence of different R_3P was investigated, and their electronic and steric properties have a comparable effect on the catalytic behavior. When Ph_3P or Cy_3P was employed as an auxiliary ligand, the activities increased up to be 10^7 g mol^{-1}(Ni) h^{-1}.

4. Experimental Section

4.1. General Considerations. All manipulations of air- and/or moisture-sensitive compounds were carried out under an atmosphere of nitrogen using standard Schlenk techniques. Solvents were refluxed over an appropriate drying agent, distilled, and degassed before using. An Et_2AlCl (1.90 mol L^{-1}) solution in toluene was purchased from Acros Chemicals. [(DME)$NiBr_2$][19] and substituted 8-nitroquinolines[14] were prepared according to literature procedures. High-purity ethylene was purchased from Beijing Yansan Petrochemical Co. and used as received. Other reagents were purchased from Aldrich, Acros, or local suppliers. Elemental analyses were performed on a Flash EA 1112 microanalyzer. IR spectra were recorded on a Perkin-Elmer System 2000 FT-IR spectrometer using KBr discs in the range 4000−400 cm^{-1}. The ^{1}H NMR spectra were recorded on a Bruker DMX-300 instrument with TMS as the internal standard. GC analysis was performed with a Varian CP-3800 gas chromatograph equipped with a flame ionization detector and a 30 m (0.25 mm i.d., 0.25 μm film thickness) CP-Sil 5 CB column.

4.2. Synthesis of Complexes 1a−12a and 1b−12b. Complexes **1a−12a** were prepared in a similar manner by using $NiCl_2 \cdot 6H_2O$. A suspension of pyridine-2-aldehyde or ketone (1.00 mmol), 8-aminoquinoline (1.00 mmol), and $NiCl_2 \cdot 6H_2O$ (1.00 mmol) in glacial acetic acid (10 mL) was refluxed for 4 h. The precipitate was collected by filtration and washed with diethyl ether (3×5 mL). Then the collected solid was redissolved in methanol, concentrated, and precipitated with diethyl ether. After washing with diethyl ether the collected solid was dried under vacuum.

Complex **1a** was obtained as a yellow powder in 55.1% yield. Anal. Calcd for $C_{15}H_{11}Cl_2N_3Ni \cdot 1.5H_2O$: C, 46.21; H, 3.62; N, 10.78. Found: C, 46.15; H, 3.51; N, 10.85. IR (KBr; cm^{-1}): 3323, 3127, 1627, 1598, 1584, 1506, 1474, 1402, 1380, 1323, 1136, 1080, 1031, 1009, 831, 769.

Complex **2a** was obtained as a yellow powder in 74.0% yield. Anal. Calcd for $C_{16}H_{13}Cl_2N_3Ni \cdot 2.5H_2O$: C, 45.55; H, 4.30; N, 9.96. Found: C, 45.54; H, 4.02; N, 10.02. IR (KBr; cm^{-1}): 3361, 3181, 1622, 1598, 1584, 1504, 1468, 1428, 1389, 1372, 1317, 1260, 1238, 1212, 1143, 1103, 1066, 1009, 834, 787.

Complex **3a** was obtained as a brown powder in 87.6% yield. Anal. Calcd for $C_{16}H_{13}Cl_2N_3Ni \cdot 2H_2O$: C, 46.54; H, 4.15; N, 10.18. Found: C, 46.21; H, 4.15; N, 10.17. IR (KBr; cm^{-1}): 3313, 3198, 1630, 1597, 1584, 1504, 1463, 1401, 1380, 1321, 1254, 1135, 1082, 1035, 1005, 834, 787.

Complex **4a** was obtained as a brown powder in 88.4% yield. Anal. Calcd for $C_{17}H_{15}Cl_2N_3Ni \cdot 2H_2O$: C, 51.05; H, 4.03; N, 10.51. Found: C, 50.79; H, 4.00; N, 10.33. IR (KBr; cm^{-1}): 3363, 3190, 1621, 1593, 1562, 1504, 1469, 1428, 1376, 1317, 1256, 1214, 1146, 1104, 1069, 1009, 834, 787.

Complex **5a** was obtained as a brown powder in 51.5% yield. Anal. Calcd for $C_{18}H_{17}Cl_2N_3Ni \cdot 2.5H_2O$: C, 48.04; H, 4.93; N, 9.34. Found: C, 48.13; H, 4.96; N, 9.23. IR (KBr; cm^{-1}): 3366, 2966, 1620, 1598, 1572, 1506, 1471, 1375, 1223, 1149, 1042, 1016, 843, 770.

Complex **6a** was obtained as a brown powder in 47.6% yield. Anal. Calcd for $C_{19}H_{19}Cl_2N_3Ni$: C, 54.47; H, 4.57; N, 10.03. Found: C, 54.97; H, 4.59; N, 10.08. IR (KBr; cm^{-1}): 3438, 3021, 2967, 2883, 1621, 1593, 1573, 1504, 1461, 1383, 1253, 1217, 1098, 1037, 861, 844, 774.

Complex **7a** was obtained as a purple powder in 88.1% yield. Anal. Calcd for $C_{19}H_{19}Cl_2N_3Ni \cdot 3H_2O$: C, 48.24; H, 5.33; N, 8.88. Found: C, 47.82; H, 5.06; N, 8.65. IR (KBr; cm^{-1}): 3350, 2963, 1602, 1507, 1475, 1443, 1366, 1233, 1132, 1014, 848, 766.

Complex **8a** was obtained as a purple powder in 84.9% yield. Anal. Calcd for $C_{20}H_{21}Cl_2N_3Ni \cdot H_2O$: C, 53.26; H, 5.14; N, 9.32. Found: C, 52.79; H, 4.84; N, 8.86. IR (KBr; cm^{-1}): 3396, 2963, 1623, 1597, 1561, 1503, 1470, 1365, 1255, 1163, 1127, 1012, 844, 768.

Complex **9a** was obtained as a brown powder in 81.3% yield. Anal. Calcd for $C_{21}H_{21}Cl_2N_3Ni \cdot 1.5H_2O$: C, 53.43; H, 5.12; N, 8.90. Found: C, 53.66; H, 5.02; N, 9.02. IR (KBr; cm^{-1}): 3327, 2927, 2850, 1620, 1596, 1571, 1502, 1475, 1446, 1375, 1299, 1259, 1221, 1150, 1104, 1025, 997, 839, 769, 607, 560, 500, 423, 375.

Complex **10a** was obtained as a brown powder in 65.4% yield. Anal. Calcd for $C_{22}H_{23}Cl_2N_3Ni \cdot MeOH$: C, 56.25; H, 5.54; N, 8.56. Found: C, 56.59; H, 5.64; N, 8.53. IR (KBr; cm^{-1}): 3434, 2926, 2851, 1620, 1594, 1570, 1503, 1445, 1382, 1255, 1160, 1032, 996, 838, 794, 768.

Complex **11a** was obtained as a brown powder in 74.6% yield. Anal. Calcd for $C_{16}H_{13}Cl_2N_3Ni \cdot 2H_2O$: C, 46.54; H, 4.15; N, 10.18. Found: C, 46.87; H, 3.85; N, 9.83. IR (KBr; cm^{-1}): 1612, 1594, 1498, 1468, 1439, 1367, 1324, 1307, 1256, 838, 781.

Complex **12a** was obtained as a brown powder in 61.2% yield. Anal. Calcd for $C_{21}H_{15}Cl_2N_3Ni \cdot 2H_2O$: C, 53.10; H, 4.03; N, 8.85. Found: C, 53.52; H, 3.81; N, 8.76. IR (KBr; cm^{-1}): 1613, 1592, 1497, 1465, 1441, 1383, 1324, 1266, 1247.

Complexes **1b−12b** were prepared in a similar manner by using (DME)$NiBr_2$. A suspension of pyridine-2-aldehyde or ketone (1.00 mmol), 8-aminoquinoline (1.00 mmol), and (DME)$NiBr_2$ (1.00 mmol) in glacial acetic acid (20 mL) was refluxed for 4 h. The precipitate was collected by filtration and washed with diethyl ether (3×5 mL). Then the collected solid was redissolved in methanol, concentrated, and precipitated with diethyl ether. After washing with diethyl ether the collected solid was dried under vacuum.

Complex **1b** was obtained as a yellow powder in 83.2% yield. Anal. Calcd for $C_{15}H_{11}Br_2N_3Ni$: C, 39.88; H, 2.45; N, 9.30. Found: C, 39.56; H, 2.64; N, 8.95. IR (KBr; cm^{-1}): 3039, 1622, 1593, 1562, 1501, 1472, 1426, 1392, 1318, 1256, 1214, 1134, 1101, 1069, 1014, 830, 776.

Complex **2b** was obtained as a yellow powder in 89.1% yield. Anal. Calcd for $C_{16}H_{13}Br_2N_3Ni \cdot H_2O$: C, 39.72; H, 3.13; N, 8.69. Found: C, 39.70; H, 3.27; N, 8.62. IR (KBr; cm^{-1}): 3361, 3181, 1622, 1598, 1584, 1504, 1468, 1428, 1389, 1372, 1317, 1260, 1238, 1212, 1143, 1103, 1066, 1009, 840, 773.

Complex **3b** was obtained as a yellow powder in 79.2% yield. Anal. Calcd for $C_{16}H_{13}Br_2N_3Ni \cdot H_2O$: C, 39.72; H, 3.13; N, 8.69. Found: C, 39.89; H, 3.26; N, 8.75. IR (KBr; cm^{-1}): 3105, 1624, 1594, 1568, 1503, 1471, 1427, 1398, 1319, 1252, 1213, 1136, 1110, 1076, 1006, 828, 779.

(19) Cotton, F. A. *Inorg. Synth.* **1971**, *13*, 160−164.

Table 10. Summary of Crystallographic Data for 3b, 4a, 6a, 6b, 10a, 10b, 11a, and 12a

	3b·3H$_2$O	**4a·H$_2$O**	**6a**	**6b**
empirical formula	$C_{32}H_{26}Br_4N_6Ni_2O_6$	$C_{17}H_{15}Cl_2N_3NiO$	$C_{19}H_{19}Cl_2N_3Ni$	$C_{19}H_{19}Br_2N_3Ni$
fw	1027.65	406.93	418.98	507.9
cryst syst	monoclinic	triclinic	monoclinic	monoclinic
space group	*P*2(1)/*n*	$P\bar{1}$	*P*2(1)/*n*	*P*2(1)/*n*
a (Å)	11.344(2)	7.4690(15)	11.434(2)	11.781(2)
b (Å)	11.117(2)	9.6646(19)	13.312(3)	13.462(3)
c (Å)	15.401(3)	12.041(2)	13.038(3)	13.021(3)
α (deg)	90	98.98(3)	90	90
β (deg)	99.16(3).	95.52(3)	111.92(3)	111.39(3)
γ (deg)	90	100.84(3)	90	90
V (Å^3)	1917.6(7)	836.1(3)	1841.0(6)	1922.7(7)
Z	2	2	4	4
D_{calcd} (g cm^{-3})	1.780	1.616	1.512	1.755
μ (mm^{-1})	5.198	1.488	1.350	5.172
T (K)	296(2)	296(2)	296(2)	296(2)
F(000)	1008	416	864	1008
θ range (deg)	2.08−25.01	1.73−27.48	2.28−27.47	2.40−27.48
no. of rflns collected	3175	6659	8165	4409
no. of unique rflns	3175	3617	4206	4409
goodness-of-fit on F^2	1.038	1.02	1.061	0.965
R	0.0955	0.0548	0.0467	0.0593
R_w	0.2570	0.1376	0.109	0.1105

	10a·MeOH	**10b**	**11a·2MeOH**	**12a·2MeOH**
empirical formula	$C_{23}H_{26}Cl_2N_3NiO$	$C_{22}H_{23}Br_2N_3Ni$	$C_{18}H_{21}Cl_2N_3NiO_2$	$C_{44}H_{36}Cl_4N_6Ni_2O_2$
fw	490.08	547.96	440.99	940.01
cryst syst	triclinic	orthorombic	triclinic	monoclinic
space group	$P\bar{1}$	*Pbca*	$P\bar{1}$	*P*2(1)/*n*
a (Å)	9.964(2)	15.456(3)	7.667(3)	8.7471(17)
b (Å)	10.764(2)	14.705(3)	9.898(4)	21.063(4)
c (Å)	13.397(3)	19.167(4)	13.088(5)	12.361(5)
α (deg)	97.85(3)	90	86.279(12)	90
β (deg)	105.45(3)	90	84.640(10)	112.42(2)
γ (deg)	117.28(3)	90	72.493(8)	90
V (Å^3)	1173.5(4)	4356.3(15)	942.3(6)	2105.3(10)
Z	2	8	2	2
D_{calcd} (g cm^{-3})	1.387	1.671	1.554	1.483
μ (mm^{-1})	1.073	4.572	1.331	1.193
T (K)	296(2)	296(2)	296(2)	296(2)
F(000)	510	2192	456	964
θ range (deg)	2.23−27.47	2.19−27.48	2.16−27.48	2.63−27.32
no. of rflns collected	8289	4990	7349	8055
no. of unique rflns	5275	4990	4253	4610
goodness-of-fit on F^2	1.092	0.77	1.075	1.096
R	0.0624	0.0328	0.0387	0.1069
R_w	0.1645	0.0392	0.0758	0.2664

Complex **4b** was obtained as a brown powder in 80.5% yield. Anal. Calcd for $C_{17}H_{15}Br_2N_3Ni$: C, 42.55; H, 3.15; N, 8.76. Found: C, 42.41; H, 3.21; N, 8.61. IR (KBr; cm^{-1}): 3367, 3193, 1619, 1593, 1562, 1504, 1469, 1428, 1376, 1317, 1256, 1214, 1146, 1104, 1069, 1009, 848, 764.

Complex **5b** was obtained as a brown powder in 72.3% yield. Anal. Calcd for $C_{18}H_{17}Br_2N_3Ni$: C, 43.78; H, 3.47; N, 8.51. Found: C, 43.38; H, 3.62; N, 8.46. IR (KBr; cm^{-1}): 3367, 3051, 2962, 1619, 1597, 1571, 1505, 1374, 1223, 1040, 841, 769.

Complex **6b** was obtained as a brown powder in 79.7% yield. Anal. Calcd for $C_{19}H_{19}Br_2N_3Ni$: C, 44.93; H, 3.77; N, 8.27. Found: C, 45.46; H, 3.96; N, 8.18. IR (KBr; cm^{-1}): 3394, 2962, 1614, 1600, 1556, 1506, 1474, 1327, 1183, 789.

Complex **7b** was obtained as a purple powder in 83.2% yield. Anal. Calcd for $C_{19}H_{19}Br_2N_3Ni$·MeOH: C, 44.49; H, 4.29; N, 7.78. Found: C, 44.34; H, 4.68; N, 8.19. IR (KBr; cm^{-1}): 3363, 2966, 1623, 1600, 1577, 1467, 1369, 1233, 1140, 749.

Complex **8b** was obtained as a purple powder in 89.4% yield. Anal. Calcd for $C_{20}H_{21}Br_2N_3Ni$: C, 46.03; H, 4.06; N, 8.05. Found: C, 46.35; H, 4.29; N, 7.71. IR (KBr; cm^{-1}): 3394, 2962, 1614, 1600, 1556, 1506, 1474, 1327, 1163, 789.

Complex **9b** was obtained as a yellow powder in 89.3% yield. Anal. Calcd for $C_{21}H_{21}Br_2N_3Ni$·0.5H_2O: C, 46.46; H, 4.08; N, 7.74. Found: C, 46.72; H, 4.05; N, 7.68. IR (KBr; cm^{-1}): 3342, 3058, 2931, 2855, 1619, 1596, 1571, 1506, 1477, 1448, 1380, 1298, 1260, 1225, 1146, 1106, 1014, 998, 839, 768.

Complex **10b** was obtained as a brown powder in 81.6% yield. Anal. Calcd for $C_{22}H_{23}Br_2N_3Ni$: C, 48.22; H, 4.23; N, 7.67. Found: C, 47.85; H, 4.25; N, 7.69. IR (KBr; cm^{-1}): 2927, 2851, 1620, 1595, 1505, 1472, 1446, 1382, 1319, 1255, 1215, 1168, 1147, 1023, 997, 958, 842, 767.

Complex **11b** was obtained as a yellow powder in 81.0% yield. Anal. Calcd for $C_{16}H_{13}Br_2N_3Ni$·H_2O: C, 39.72; H, 3.13; N, 8.69. Found: C, 39.42; H, 3.21; N, 8.68. IR (KBr; cm^{-1}): 3273, 3062, 1595, 1500, 1473, 1445, 1369, 1262, 1248, 1021, 835, 759, 765.

Complex **12b** was obtained as a yellow powder in 83.4% yield. Anal. Calcd for $C_{21}H_{15}Br_2N_3Ni$·1.5H_2O: C, 45.46; H, 3.27; N, 7.57. Found: C, 45.59; H, 3.22; N, 7.69. IR (KBr; cm^{-1}): 3394, 3050, 1610, 1595, 1499, 1467, 1386, 1329, 1267, 1249, 839, 792, 769, 708.

4.3. Procedure for Oligomerization of Ethylene. Ethylene oligomerization at 1 atm of ethylene pressure was carried out as follows: the catalyst precursor was dissolved in toluene in a Schlenk tube, and the reaction solution was stirred with a magnetic stir bar under ethylene atmosphere (1 atm) with the reaction temperature being controlled by a water bath. Et_2AlCl and the solution of R_3P were added by a syringe. After the reaction was carried out for the required period, the reactor was cooled in an ice−water bath. A

small amount of the reaction solution was collected and terminated by the addition of 10% aqueous hydrogen chloride. The organic layer was analyzed by gas chromatography (GC) for determining the composition and mass distribution of oligomers obtained.

High-pressure ethylene oligomerization was performed in a stainless steel autoclave (0.5 L capacity) equipped with gas ballast through a solenoid clave for continuous feeding of ethylene at constant pressure. A 100 mL amount of toluene containing the catalyst precursor was transferred to the fully dried reactor under a nitrogen atmosphere. The required amount of cocatalyst (Et_2AlCl) was then injected into the reactor using a syringe. As the prescribed temperature was reached, the reactor was pressurized to the desired pressure. After the reaction mixture was stirred for the desired period of time, the reaction was stopped without ethylene inputting. The autoclave was cooled in an ice−water bath, then the pressure was released. A small amount of the reaction solution was collected and terminated by the addition of 10% aqueous hydrogen chloride. The organic layer was analyzed by gas chromatography (GC) for determining the composition and mass distribution of oligomers obtained.

4.4. X-ray Crystallographic Studies. Single-crystal X-ray studies for complexes **3b**, **4a**, **6a**, **6b**, **10a**, **10b**, and **12a** were carried out on a Rigaku R-AXIS Rapid IP diffractometer with graphite-monochromated Mo Kα radiation ($\lambda = 0.71073$ Å) at 296(2) K. Intensity data for crystals of **11a** were collected on a Bruker SMART 1000 CCD diffractometer with graphite-monochromated Mo Kα radiation ($\lambda = 0.71073$ Å) at 296(2) K. Cell parameters were obtained by global refinement of the positions of all collected reflections. Intensities were corrected for Lorentz and polarization effects and empirical absorption. The structures were solved by direct methods and refined by full-matrix least-squares on F^2. All non-hydrogen atoms were refined anisotropically. All hydrogen atoms were placed in calculated positions. Structure solution and refinement were performed by using the SHELXL-97 package.[20] Crystal data and processing parameters for complexes **3b**, **4a**, **6a**, **6b**, **10a**, **10b**, **11a**, and **12a** are summarized in Table 10 while molecular structures and selected bond lengths and angles of complexes **6b**, **10b**, and **12a** are given in the Supporting Information.

Acknowledgment. This project was supported by NSFC No. 20473099. K.W. was supported by a DAAD postdoctoral fellowship.

Supporting Information Available: Crystallographic data for **3b**, **4a**, **6a**, **6b**, **10a**, **10b**, **11a**, and **12a** along with the descriptions of molecular structures of **6b**, **10b**, and **12a**. This material is available free of charge via the Internet at http://pubs.acs.org.

OM700440V

(20) Sheldrick, G. M. *SHELXTL-97*, Program for the Refinement of Crystal Structures; University of Göttingen: Germany, 1997.